The prediction of the complex characteristic acoustic impedance of porous materials

David James Larner[1]; John Laurence Davy[2]

[1,2] RMIT University, GPO Box 2476 Melbourne, VIC 3001 Australia

ABSTRACT

Modeling the complex characteristic acoustic impedance and complex wavenumber of porous materials allows the prediction of the complex specific acoustic impedance of a system consisting of porous absorbers and air cavities in front of a rigid surface. By using the transfer matrix method, the complex characteristic acoustic impedance and complex wavenumber of a porous material can be predicted by using the measured complex specific acoustic impedance of two different systems of the porous material and an air cavity, performed in a two-microphone impedance tube. Depending on the method, the material can be measured with either a rigidly terminated back plate at the back of the material, or a rigidly terminated air cavity at the back. This paper looks at why predictions using the single and double thickness method break down for thinner, less dense materials.

Keywords: Impedance, wavenumber, porous materials I-INCE Classification of Subjects Number(s): 72.7.2

1. INTRODUCTION

Predictions of the complex characteristic acoustic impedance and complex wavenumber of porous materials are useful tools to help predict the complex specific acoustic impedance of multi-layered systems. By knowing the thickness, complex wavenumber and complex characteristic acoustic impedance of a material layer, the specific acoustic impedance at the face of the layer can calculated, and subsequent layers can be calculated using the transfer matrix method, which allows for the absorption coefficient of the system to be calculated. Three prediction methods have been investigated; the Dunn and Davern (1) method which derives the characteristic impedance of a material by comparing specific acoustic impedance of the single and double thickness of the same material with no air cavity; the Utsuno *et al.* (2) method which compares the specific acoustic impedance of a finite thick material with two different air cavity depths behind it, and a third method; which is the second method when one of the air cavities has zero depth.

2. Theory

2.1 Prediction of the complex characteristic impedance using the Dunn and Davern method

Dunn and Davern developed a method for predicting the complex characteristic acoustic impedance of porous materials Z_c by deriving equations based on the prediction of the complex specific acoustic impedance Z_0 using the transfer matrix method;

$$Z_0 = Z_c \frac{Z_1 \cos(\tilde{k}d) + jZ_c \sin(\tilde{k}d)}{Z_c \cos(\tilde{k}d) + jZ_1 \sin(\tilde{k}d)} \quad (1)$$

where Z_1 is the complex specific acoustic impedance of the previous layer, $\tilde{k}$ is the complex

[1] david.larner@rmit.edu.au
[2] john.davy@rmit.edu.au

wavenumber and d is the thickness of the porous material.

By dividing Z_1 through this equation, and then setting $Z_1 = \infty$ because in this case, Z_1 is the impedance of the rigidly terminated back plate, Equation 1 becomes;

$$Z_0 = -jZ_c \cot(\tilde{k}d) \tag{2}$$

Using this formula, Dunn and Davern stated that when the porous material is doubled, the complex specific acoustic impedance becomes;

$$Z_{02d} = -jZ_c \cot(2\tilde{k}d) \tag{3}$$

Equations 2 and 3 can be solved simultaneously to obtain both Z_c and $\tilde{k}$.

$$Z_c = \sqrt{Z_0(2Z_{02d} - Z_0)} \tag{4}$$

$$\tilde{k} = \frac{j}{2d} \ln \frac{Z_0 + Z_c}{Z_0 - Z_c} \tag{5}$$

2.2 Prediction of the complex characteristic impedance using the Utsuno *et al*. method

Utsuno *et al*. also developed the prediction of the complex characteristic acoustic impedance and complex wavenumber by using the transfer matrix method shown in Equation 1. However, this prediction method is more complicated, as it uses complex specific acoustic impedances of porous materials with different air cavity depths behind the sample.

$$Z_c = \sqrt{\frac{Z_0 Z_0'(Z_1 - Z_1') - Z_1 Z_1'(Z_0 - Z_0')}{(Z_1 - Z_1') - (Z_0 - Z_0')}} \tag{6}$$

$$\tilde{k} = \frac{j}{2d} \ln\left(\frac{Z_0 + Z_c}{Z_0 - Z_c}\frac{Z_1 - Z_c}{Z_1 + Z_c}\right) = \frac{j}{2d} \ln\left(\frac{Z_0' + Z_c}{Z_0' - Z_c}\frac{Z_1' - Z_c}{Z_1' + Z_c}\right) \tag{7}$$

where the dashed and undashed symbols denote two different air cavity depths.

Z_1 and Z_1' denote the specific acoustic impedance of the air cavity:

$$Z_1 = -j\rho_0 c \cot(kD) \tag{8}$$

$$Z_1' = -j\rho_0 c \cot(kD') \tag{9}$$

where $\rho_0 c$ is the characteristic impedance of air, k is the wavenumber of air, and D is the depth of the air cavity. It can be seen in Equation 6 that the difference between the air cavity impedances is important. Therefore, it was important to state that the air cavity impedances should be as different as possible.

2.3 Modification of the Utsuno *et al.* prediction method

To gain more complex characteristic acoustic impedance predictions of various porous materials, a combination of the two above prediction methods was used. One of the air cavity depth measurements was substituted with measurements performed when the material was backed by a rigid backing, making the specific acoustic impedance of $Z_1' = \infty$. By substituting this into Equation 6 and 7, the complex characteristic acoustic impedance and complex wavenumber became;

$$Z_c = \sqrt{Z_1(Z_0 - Z_0') + Z_0 Z_0'} \tag{10}$$

$$\tilde{k} = \frac{j}{2d}\ln\left(\frac{Z_0' + Z_c}{Z_0' - Z_c}\right) \quad (11)$$

In total, seven predictions of the specific characteristic acoustic impedance can be made from six measurements of single and double thickness materials.

Table 1: Seven predictions used to calculate the specific characteristic acoustic impedance and complex wavenumber

Method	Equations used
Dunn – Davern	Equations 4 & 5
Single layer Utsuno	Equations 8 & 9
Double layer Utsuno	Equations 8 & 9
Single Utsuno modification: compare no air gap & quarter wavelength air gap	Equations 10 & 11
Single Utsuno modification: compare no air gap & half wavelength air gap	Equations 10 & 11
Double Utsuno modification: compare no air gap & quarter wavelength air gap	Equations 10 & 11
Double Utsuno modification: compare no air gap & half wavelength air gap	Equations 10 & 11

3. Results

Four materials were used to predict the complex characteristic acoustic impedance and complex wavenumber. These materials are shown in Table 1:

Table 2: Materials measured in two-microphone impedance tube

Material	Flow Resistance (MKS Rayl)	Thickness (mm)	Density (kg.m^{-3})
Foam	148	11.8	29
Polyester	334	25.65	795
Polyester	742	50.9	831
Glass Wool	1546	49.6	396

Each of these materials were measured in both the low and high frequency two-microphone impedance tubes, with both the single and double thickness samples measured against the back plate, and with a 50 and 100 mm or a 12.5 and 25 mm air cavities for the low and high frequency measurements respectively. From these six measurements, seven predictions can be made in each of the frequency ranges. The reasoning behind selecting these air cavity depths was due to the fact that these depths are slightly below the quarter-wavelength $L_{\frac{\lambda}{4}}$ and half-wavelength $L_{\frac{\lambda}{2}}$ lengths of 53.6 & 107.2 mm and 26.8 & 53.6 mm for the maximum low (1600 Hz) and high frequency (6400 Hz) measurements f_{max} respectively, as shown below in Equations 12 and 13. At these lengths, the impedance of the air cavity is close to 0 and ∞ respectively, therefore giving the largest possible difference in air cavity impedances.

$$L_{\frac{\lambda}{4}} = \frac{c}{2f_{max}} \tag{12}$$

$$L_{\frac{\lambda}{2}} = \frac{c}{f_{max}} \tag{13}$$

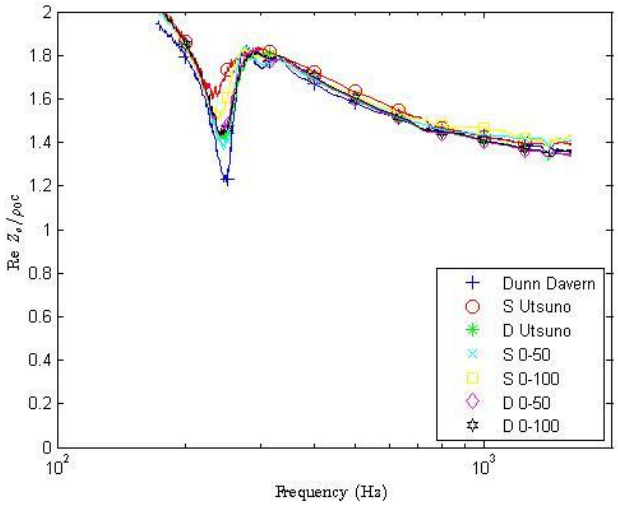

Figure 1: The normalized low frequency real characteristic acoustic impedance of the thicker polyester sample. S and D denote a single or double thickness material respectively. The last four predictions show the Equation 10 method, where the two numbers represent the air cavity depths (mm) of the dashed and undashed series respectively.

In Figure 1, it can be seen that with the seven prediction methods, there was very good agreement over the low frequency range. This shows that so far, there is no failure in the prediction of the complex characteristic acoustic impedance for this material; however, it does break down with the other materials.

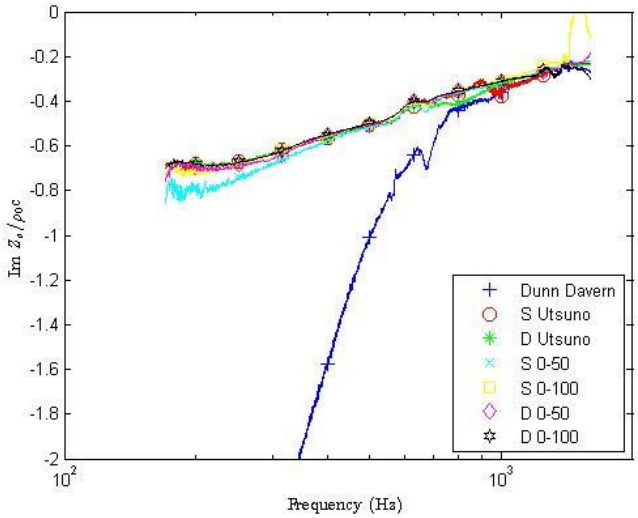

Figure 2: The normalized low frequency imaginary characteristic acoustic impedance of the foam sample. S and D denote a single or double thickness material respectively. The last four predictions show the Equation 10 method, where the two numbers represent the air cavity depths (mm) of the dashed and undashed series respectively.

Above in Figure 2, the Dunn and Davern method for predicting the complex characteristic acoustic impedance breaks down. As this is the only prediction method that breaks down in this material, the material was measured again, with a similar output in the complex specific acoustic impedance, thus retaining similar values of the complex characteristic acoustic impedance. This error will be investigated later.

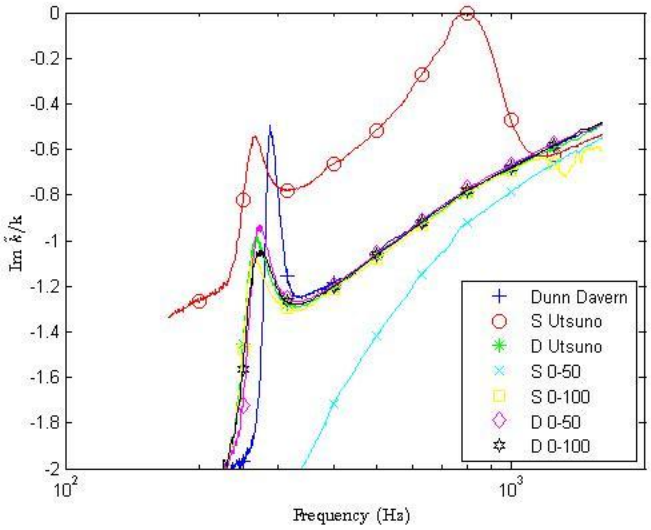

Figure 3: The normalized low frequency imaginary wavenumber of the thin polyester sample. S and D denote a single or double thickness material respectively. The last four predictions show the Equation 10 method, where the two numbers represent the air cavity depths (mm) of the dashed and undashed series respectively.

The complex wavenumber was also predicted for the materials, with some success and some errors. Above in Figure 3, it can be seen that the majority of predictions are very similar to each other, which strengthens these predictions. However, there are a few outliers, particularly with two out of the three single layer predictions.

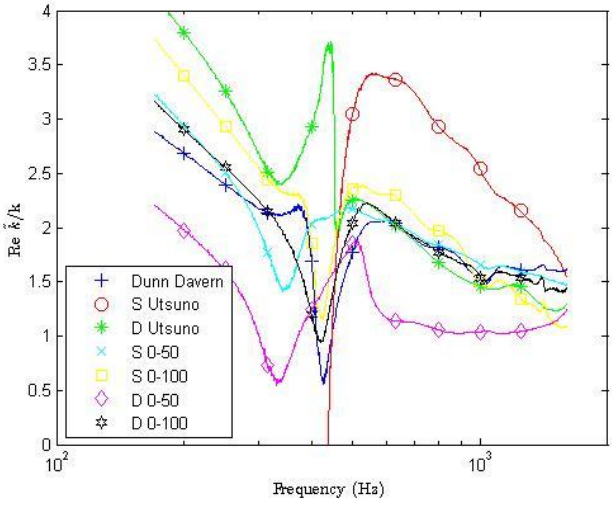

Figure 4: The normalized low frequency real wavenumber of the glass wool sample. S and D denote a single or double thickness material respectively. The last four predictions show the Equation 10 method, where the two numbers represent the air cavity depths (mm) of the dashed and undashed series respectively.

For some materials, most of the predictions can give a range of results. In Figure 4 from 500 Hz upwards, the majority of predictions of the real part of the wavenumber for glass wool appear to agree with each other more. However, there are fluctuations below 500 Hz, especially with the single sample Utsuno *et al.* method. As these values dip into the negative value region, this means that the phase constant is negative, which makes no physical sense as the rest of the predictions are in the positive domain. These measurements were redone, and similar predicted outputs for the wavenumber were present. One positive is that it appears these values converge at frequencies above 2000 Hz, so predictions using high frequency two microphone impedance tube measurements were calculated.

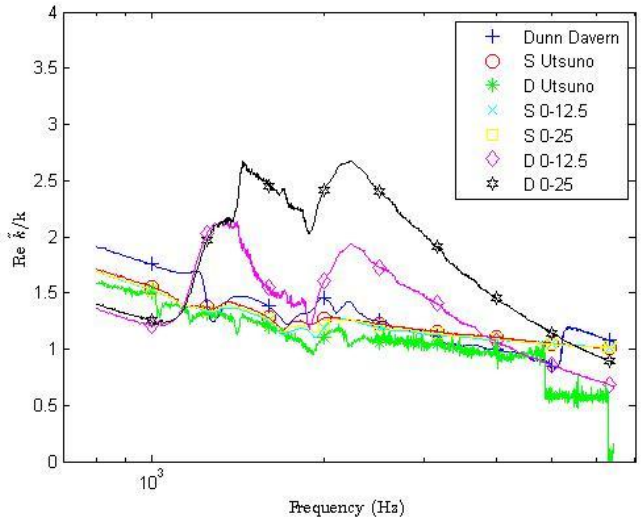

Figure 5: The normalized high frequency real wavenumber of the glass wool sample. S and D denote a single or double thickness material respectively. The last four predictions show the Equation 10 method, where the two numbers represent the air cavity depths (mm) of the dashed and undashed series respectively.

In the higher frequencies, the majority of the prediction methods converge together, as shown in Figure 5. Again, there are outliers, with all outliers having something in common, having the double thickness samples in the prediction. The thickness of the double layered glass wool of 99.2 mm could be too thick for these particular predictions.

4. Discussion

One of the main points of discussion is why does some of the prediction methods break down for some cases and not others. In the foam case, the Dunn and Davern method breaks down, even after re-measurement. By taking a closer look at Equations 2 and 3, if $\tilde{k}d \ll 1$, $\tan(\tilde{k}d) \approx \tilde{k}d$, then these Equations become;

$$Z_0 = \frac{-jZ_c}{\tilde{k}d} \tag{14}$$

$$Z_{02d} = \frac{-jZ_c}{2\tilde{k}d} \tag{15}$$

If these values are used in Equations 4 and 5, Z_c and $\tilde{k}$ are equal to 0. This problem is due to the $2Z_{02d} - Z_0$ term in Equation 4. Because both Z_{02d} and Z_0 are proportional to Z_c, Z_c does not affect the relative standard deviation of $2Z_{02d} - Z_0$. Thus Z_c is assumed to be equal to one in the following calculations. From Equation 2, the mean values of Z_{02d} and Z_0 are;

$$\overline{Z_0} = \cot(\tilde{k}d) \tag{16}$$

$$\overline{Z_{02d}} = \cot(2\tilde{k}d) \tag{17}$$

The relative standard deviations of Z_0 and Z_{02d} are assumed to be the same where this value is denoted by x

$$\sigma_{Z_0}{}^2 = x^2|\overline{Z_0}|^2 \tag{18}$$

$$\sigma_{Z_{02d}}{}^2 = x^2|\overline{Z_{02d}}|^2 \tag{19}$$

The relative standard deviation of $2Z_{02d} - Z_0$ is

$$\frac{\sigma_{2Z_{02d}-Z_0}}{|\overline{2Z_{02d} - Z_0}|} = \frac{x}{y} \tag{20}$$

where the divisor y is given by

$$y = \frac{|\overline{2Z_{02d} - Z_0}|}{\sqrt{4|\overline{Z_0}|^2 + |\overline{Z_{02d}}|^2}} \tag{21}$$

The smaller the value of the divisor y, the more the relative standard deviation is increased. This value needs to be compared to $|\tilde{k}d|$, as this will show if the material is thick enough to be used in the Dunn and Davern prediction method. To calculate $|\tilde{k}d|$, the angle ϑ must first be calculated:

$$\vartheta = \arctan\left[\frac{Re(\tilde{k}d)}{Im(\tilde{k}d)}\right] \tag{22}$$

which allows the calculation of $|\tilde{k}d|$;

$$|\tilde{k}d| = \frac{j\tilde{k}d}{e^{j\vartheta}} \tag{23}$$

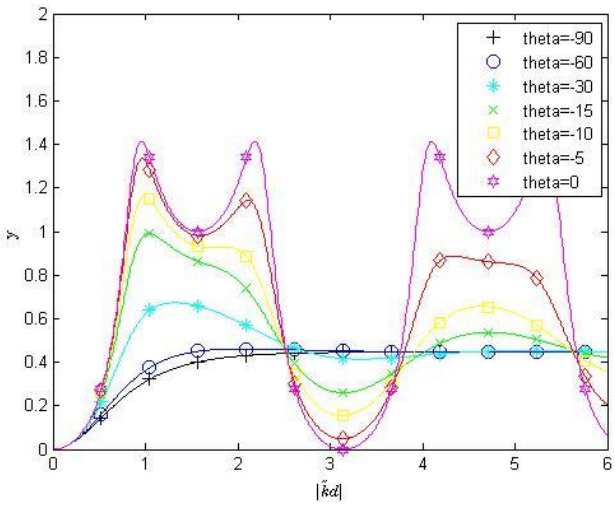

Figure 6: Plot of y vs. $|\tilde{k}d|$ at various ϑ values

In Figure 6 shows what the common value x of the relative standard deviation needs to be divided by, in order to obtain the relative standard deviation of $2Z_{02d} - Z_0$. This is assuming that the relative standard deviations of both $2Z_{02d}$ and Z_0 are the same. Below in Table 2 shows each of the materials used in the predictions, with their corresponding ϑ and $|\tilde{k}d|$ values. It can be seen that the foam case has a very low $|\tilde{k}d|$ value, which satisfies Equations 14 and 15. By looking at Figure 6, the value of

y is very small for the foam case, which causes an increase in the relative standard deviation of $2Z_{02d} - Z_0$. Therefore it can be stated that for materials with low $|\tilde{k}d|$ values, the prediction of the complex characteristic acoustic impedance and complex wavenumber can fluctuate due to the material being too thin. Therefore, the value of $|\tilde{k}d|$ should be greater than 0.7.

Table 3: Materials used in the predictions with the corresponding ϑ and $|\tilde{k}d|$ values

Material	ϑ	$\lvert\tilde{k}d\rvert$
Foam	-15°	0.6
Polyester	-17°	1.1
Polyester	-21°	2.2
Glass Wool	-29°	2.7

5. CONCLUSIONS

By comparing the seven prediction methods against each other, a quantitative prediction value of the complex characteristic acoustic impedance and complex wavenumber of porous materials can be determined. However, for some materials, these methods can break down. The Dunn and Davern method was analyzed, and it was determined that the value of $|\tilde{k}d|$ for these materials should be above 0.7. It can be recommended that for the Utsuno *et al.* method that the air cavity depths should be just under the quarter-wavelength and half-wavelength depths, as this will provide the largest difference in air cavity impedance without any resonances.

6. REFERENCES

1. Dunn IP, Davern WA. Calculation of acoustic impedance of multi-layer absorbers. Applied Acoustics. 1986;19(5):321-34.

2. Utsuno H, Tanaka T, Fujikawa T, Seybert AF. Transfer function method for measuring characteristic impedance and propagation constant of porous materials. The Journal of the Acoustical Society of America. 1989;86(2):637-43.